

BEHAVIOR OF THE CO₂ INJECTION WELL AND THE NEAR WELLBORE DURING CARBON DIOXIDE INJECTION IN SALINE AQUIFERS

Mohamed AZAROUAL¹, Laurent ANDRE¹, Yannick PEYSSON², Jacques PIRONON³, Daniel BROSETA⁴,
Fabien DEDECKER⁵, Patrick EGERMANN⁶, Jean DESROCHES⁷, Joëlle HY-BILLIOT⁸

¹ BRGM, Water Division, 3 Avenue Claude Guillemin, BP 36009, F-45060 ORLEANS Cedex 2 France

² IFP Energies nouvelles, 1-4 avenue de Bois Préau, 92852 Rueil-Malmaison Cedex - France

³ Université de Lorraine, CNRS, G2R laboratory, BP 70239, 54506 Vandœuvre-lès-Nancy, France

⁴ UMR 5150, LFCR, Université de Pau & Pays Adour, BP 1155, 64013 PAU Cedex, France

⁵ ITASCA Consultants, S.A.S., 64 Chemin des Mouilles, 69130 ECULLY, France

⁶ GDF SUEZ, STORENGY, 12 rue Raoul Nordling, 92270 Bois Colombes, France

⁷ SCHLUMBERGER, Etudes et Productions Schlumberger, SRPC, 1 rue Henri Becquerel, 92142 Clamart, France

⁸ TOTAL E&P, DGE/SCR/RD/MGR, Avenue Larribau, 64018 PAU CEDEX, France

e-mail: m.azaroual@brgm.fr; l.andre@brgm.fr; yannick.peysson@ifpen.fr ; jacques.pironon@univ-lorraine.fr; daniel.broseta@univ-pau.fr; f.dedecker@itasca.fr; patrick.egermann@storengy.com; JDesroches1@slb.com; Joelle.HY-BILLIOT@total.com.

ABSTRACT

The project "*ProchePuits*" ("Near Wellbore"), co-funded by the French National Agency for Research (ANR), started in December 2007 and ended in May 2011. The project consortium included three companies (TOTAL, Schlumberger, and GDF-Suez), two applied research centers (BRGM and IFP Energies Nouvelles), two academic research laboratories (CNRS and Université de Lorraine) and a SME (ITASCA). The main processes studied were: (i) physical behavior of flowing fluids in the well and their impacts on the bottomhole T-P conditions, (ii) thermo-kinetic effects on the petrophysical and physico-chemical processes, (iii) dryout of the near-wellbore porous media and reactivity of highly evaporated residual brines retained by capillary and osmotic forces in the pores, and (iv) petrophysical and geomechanical impacts of coupled processes.

The understanding of these phenomena, based on laboratory experiments and numerical modeling, enabled a better interpretation of the coupled processes involved and the development of advanced concepts for CO₂ storage in saline aquifers. The project demonstrates, that injection of large quantity of CO₂ in deep saline aquifers will lead to a strong water desaturation of the near wellbore because of drying. In this context, drying can precipitate the salt in the aquifer water, leading to injectivity alteration due to permeability decrease.

Numerical modeling that couples hydraulic and thermal processes was shown to be able to simulate the observed evolution of liquid and gas saturations, and to estimate the salt depositions. Our numerical-simulation approaches were validated against laboratory experiments in controlled conditions, allowing the determination of the most important parameters for injectivity design (porosity, relative permeability and capillary pressure curves, etc.). The experimental observations, conducted at the centimeter scale, were up-scaled in order to, first extrapolate the results at the near wellbore scale, and then to forecast the impact of CO₂ injection on the petrophysical properties of the host rock.

Finally, our results allow making recommendations and risk analyses with respect to the injectivity for CO₂ for geological storage in an aquifer. The injection flow rates, as well as optimum pressure and temperature in wells, can then be determined to avoid damage in the near wellbore zone and maintain injectivity during the operational life of the well.

INTRODUCTION

The "*Near Wellbore*" project was focused on the study of key physical, physicochemical, and thermo-kinetic phenomena occurring in the well and the near-wellbore domain. The understanding of these phenomena, based on scientific and technical knowledge, will reduce uncertainties related to injectivity and numerical-simulation

predictions regarding the sustainability and security of CO₂ storage. This knowledge will also identify ranges for CO₂ storage-capacity estimates within saline aquifers.

Indeed, it is now established that the amount and quality of injected CO₂ play a key role in the preservation of reservoir injectivity, and on the number and type of required injection wells. On the other hand, depth, location, temperature and pressure conditions, and petrophysical characteristics of the targeted reservoir—as well as the quality of the cap rock—are parameters that must be characterized because of their influence on the required number of wells, on the evolution of injectivity, and on the technical management of pressure conditions at the wellhead and at the bottom of the well. Additionally, the multiphase area that develops nearing the vicinity of the well is a very sensitive, highly reactive zone, where numerous coupled processes have been identified, including hysteretic behaviors. This region may also play a key role during the CO₂ injection phase, which can include repeated injection cessations and restarts.

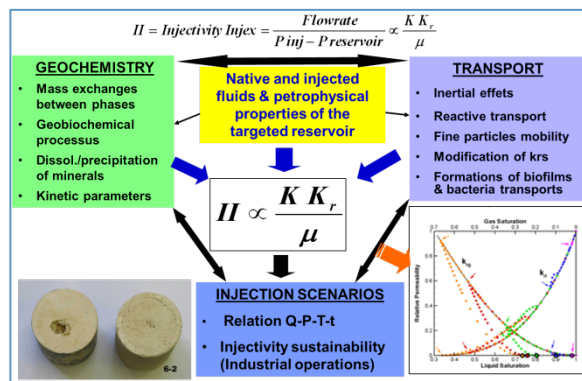


Figure 1. Key coupled processes to integrate in numerical tools for studying injection scenarios, based on controlling relative permeabilities and interfacial mechanisms of mass and heat transfer between phases.

In summary, the integration of the empirical macroscopic parameter defined as the *injectivity index*, II , (Figure 1) is the key condition of success for a Geological Carbon Sequestration (GCS) operation. This parameter expresses the behavior of the reservoir under imposed P-T-Q-t conditions, i.e., injection pressure (P), temperature (T), flow (Q) and their time evolution (t). As illustrated in Figure 1, II primarily depends

on the evolution of the relationship between water saturation (S_w) and relative permeability (K_r). This relationship depends, in turn, on the properties of the injected fluids and on the characteristics of the target reservoir rock (biochemical and geochemical reactivity, initial petrographic and hydrodynamic properties, etc.).

MULTIPHASE REACTIVE TRANSPORT AND NEARWELLBORE BEHAVIOR

Based on recent numerical and experimental simulations, the near-well injection zone is identified to be particularly impacted by supercritical CO₂ injection, and is the most sensitive area. This area (André et al., 2007; 2010), is where chemical (e.g., mineral dissolution/precipitation) and physical (e.g., temperature, pressure and gravity) phenomena have a major impact on porosity and permeability, and thus, in the end, on well injectivity.

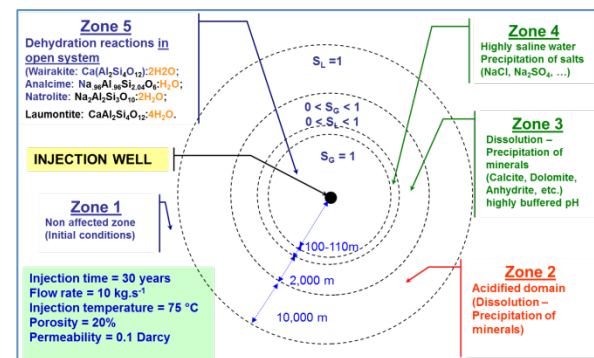


Figure 2. Typical fictive radii of the processes occurring in the near well region after a continuous injection of CO₂ over 30 years with a flow rate of 1 Mm³/y (André et al., 2007; Gaus et al., 2008).

Figure 2 represents the simulation result from two-phase reactive transport (CO₂—initially porous carbonate rock saturated with water) using TOUGHREACT (Xu et al., 2004), showing the individualization and succession of five major zones of specific physical and physico-chemical properties around the injection well. These zones have the following characteristics:

- Zone 1 (initial unperturbed state): the porous medium contains only the initial aqueous solution. The pores are saturated with water (initial state) under conditions of thermody-

namic equilibrium between minerals of the rock matrix and pore water.

- Zone 2 (monophasic acidified zone): pH decreases due to dissolution of CO₂ (forming carbonic acid H₂CO₃) in the aqueous phase. The porous medium is still saturated with water. This is a more acidic front before the arrival of the supercritical CO₂ phase. This solution at lower pH is aggressive for most of the porous matrix minerals, including carbonates and to a lesser degree aluminosilicates.
- Zone 3 (multiphase zone): the pores of the porous medium contain two phases, namely the aqueous phase and supercritical CO₂. The pH and composition of the aqueous phase and slight change in water saturation continues, with a drying trend of the rock, creating conditions for capillarity.
- Zone 4 (dried zone): pH and ionic strength increase sharply due to the drying. This produces a strong tendency in the system toward reactive mass exchange processes between major phases (residual water–supercritical CO₂–minerals). Pore solutions become highly saline, with ionic-strength values of about 7 to 7.5 (equivalent mol / kg H₂O) although the initial aqueous solution was only at 0.1 (Zone 1).
- Zone 5 (extreme conditions of capillarity and dehydration reactions): the aqueous phase is removed and the porous medium contains only supercritical CO₂, along with a small quantity of metastable and capillary water in the fine pores and microcracks.

The various physical and physicochemical phenomena that predominated in each zone were analyzed separately in the framework of the “*Near Wellbore*” project, by implementing new measurement techniques and some new theoretical approaches. The integration of results from different disciplines helps us understand multiphase reactive transport inducing heat and mass transfer between phases.

The CO₂ injection well behavior: a “Pseudo” steady-state calculation example

This test case, jointly run by Total and Schlumberger, consists of a single-cased off-shore well, located in a shallow water zone (300 m depth).

The well is vertical, and its total depth is 1000 m. Boundary conditions (pressure, temperature, and volumetric flow rate) are set at the wellhead. The injection temperature is set at 5°C, while the injection pressure is set at 100 bars. Several volumetric flow rates are considered: 500 t/day, 1000 t/day, 2000 t/day, and 2750 t/day. The far-field temperature in the formation varies linearly from 5°C at wellhead (0 m) to 21°C at 1000 m. The geological formation was made of limestone and sandstone, but since the thermal properties were not available, we chose the same parameters for both layers, assuming that this approach would not change the results significantly.

This example was tested using PipeSIM (developed by Schlumberger) and PROSPER (developed by Total). Each software involves different theoretical approaches and practical assumptions. PipeSIM performs steady-state calculations exclusively, in contrast to PROSPER, which produces results at $t = 10$ days, 100 days, and 1000 days from the beginning of injection. The longer times are fairly large, and probably sufficiently close to steady state to allow a meaningful comparison of the results of the two simulators. The codes yielded different results. Note that the pressure-versus-temperature curve along the well calculated with PipeSIM looks unconvincing (Figure 3): a substantial change in the slope occurs when the pressure exceeds a value ranging between 72 and 76 bars for the cases investigated (depending on the volumetric flow rate and the equation of state (EOS) considered for CO₂).

The simulations carried out with PROSPER use the Peng-Robinson EOS (Peng-Robinson, 1976) to model the behavior of CO₂. The simulator described here (NEW SIMULATOR) uses the Span-Wagner EOS (Span-Wagner, 1996). PipeSIM calculations are run alternatively using these two equations of state.

In earlier simulations, the convective heat transfer coefficient between tubing and the fluid inside it was considered constant ($11 \text{ W}\cdot\text{m}^{-2}\cdot\text{K}^{-1}$) all along the well. This is not the case under realistic conditions: the heat transfer coefficient is usually dependent on numerous parameters evolving with depth and time (e.g., the fluid velocity, density, viscosity). The heat exchange between the fluid and the pipe is often expressed by means of a correlation relating the Reynolds,

Prandtl, and Nusselt numbers of the flow. In the current version of this new simulator, the correlation implemented is that of Gnielinski (Incropera, 2001).

The temperature vs. pressure curves associated with each case are presented in Figure 3. The numbers in the caption are the flow-rate values (in ton/day), while the two-letter acronyms ‘SW’ and ‘PR’ denote respectively ‘Span-Wagner’ and ‘Peng-Robinson’ (the equations of state of CO₂ used for the current case).

The present simulator is denoted ‘NEWSIM’ in the caption (‘PipeSIM’ and ‘PROSPER’ are self-explanatory). Figure 3 shows that the NEWSIM results are much closer to those from PROSPER than those from PipeSIM. In particular, the associated curves do not exhibit the unexplainable change in slope mentioned above, which tends to suggest a lack of coherence in the PipeSIM results. NEWSIM predicts a temperature 10 to 13% lower than PROSPER, and a pressure 4 to 5% higher.

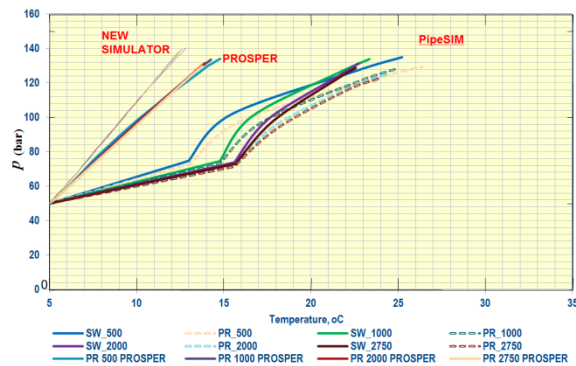


Figure 3. Pressure vs. temperature curves obtained with the three simulators, considering four flow rates and two different equations of states.

To summarize, these discrepancies can be explained by one or a combination of the following reasons:

- The use of the Span-Wagner (1996) EOS instead of the Peng-Robinson (1976) EOS. This trend is similar to that observed in the PipeSIM results when one switches from one EOS to the other: the bottom-hole temperature sustains a 4% to 5% relative decrease, while the bottom-hole pressure increases 4 to 5%.

- The use of a variable CO₂/tubing heat transfer coefficient—described by the Gnielinski’s correlation; see Incropera (2001)—instead of a constant one.

The near wellbore dynamics

As shown in Figure 2, the desiccation of the porous medium appears to be a major phenomenon with various consequences, such as salt precipitation (Peysson et al., 2010), the consequent modification of the local geomechanical constraints, modification of internal forces, and the impact of injected fluids on interfacial tensions, including capillary/osmotic phenomena. Desiccation of porous media submitted to gas injections is a well-known process in laboratory studies (Mahadevan, 2005; Mahadevan et al., 2007) and field (Kleinitz et al., 2003) scales. This process began being taken into account only recently in the modeling of CO₂ storage in deep saline aquifers (André et al., 2007; Zeidouni et al., 2009).

First, the massive and continuous injection of CO₂ in a saturated porous medium involves water displacement and evaporation: mobile water is removed by the injected dehydrated supercritical CO₂, enabling a two-phase flow system (brine–CO₂). Finally, the immobile residual water entrapped in pores or distributed on grain surface as a thin film comes into contact with the flowing dry CO₂ (i.e., with very low water vapor pressure). Consequently, a continuous and extensive evaporation process leads to both a drying front moving into the medium and the precipitation of salts and possibly secondary minerals occurring in residual brines.

This study investigated the consequences for permeability degradation of a porous medium potentially influenced by desiccation through the petrophysical properties of different subsystems. Experimental evaluations of brine drying are conducted (at the laboratory scale) on centimeter plugs of different materials. These experiments were then interpreted using a numerical modeling approach coupling hydraulic and thermal processes able to simulate the evolution of liquid and gas saturations in space and time. A very fine discretization of the plugs allowed capturing the continuous evolution of water and gas profiles in the porous medium and estimating the

liquid saturation and permeability evolution during the drying process.

Gas-injection experiments were performed on two materials:

- a low-permeability sandstone ("Grès de Môlière" $\Phi=14.0\%$ and $K_0=8\ \mu\text{D}$) in order to have better experimental control of the pressure, to limit the gas flow rate, and to increase the capillary effects that play a key role in drying processes,
- a high-permeability sandstone ("Grès des Vosges" $\Phi=21.8\%$ and $K_0=60\ \text{mD}$) in order to study a rock with properties close to the ones found in targeted reservoirs for CO_2 storage.

Sandstones samples 6 cm in length, initially saturated with brine (salinity of $160\ \text{g L}^{-1}$), were placed in storage conditions (80°C – 120°C –50 bars) and in a cell transparent to x-rays. Dry gas (nitrogen) was injected into the fully saturated core plugs (Figure 4). Four long pressure stages were imposed to progressively desaturate the rock plug. The local water saturation in the sample was measured with x-ray attenuation techniques. Pressure differences and outlet gas flow rates were monitored during the experiment. The system evolved until complete drying occurs. The experiments were performed at 90 and 120°C with the "Grès de Môlière" samples, and at 90°C with the "Grès des Vosges" core.

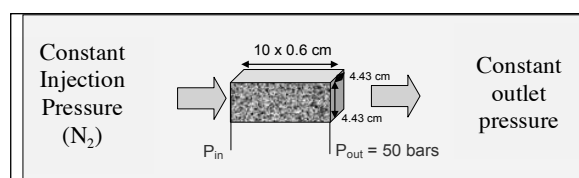


Figure 4. Experimental procedure to investigate the drying out of the core under a continuous flux of nitrogen.

Numerical simulation of multiphase flow and dryout (lab scale)

The TOUGH2 simulator (Pruess et al., 1999) with the EOS7C module (Oldenburg et al., 2004) was used for all simulations in this study (core experiments and field scale). This code couples thermal and hydraulic processes and is applicable to one-, two-, or three-dimensional geologic systems with physical heterogeneity. The EOS7C is a fluid-property module developed specifically to deal with mixtures of non-

condensable gases (like CO_2 or N_2) and methane. It can be used to model isothermal or non-isothermal multiphase flow in water/brine/ CH_4 /(CO_2 or N_2) systems.

Our modeling approach consisted of simulating the injection of nitrogen into a plug fully saturated with water. This problem of two-phase Darcy flow is solved using relative permeability and capillary pressure curves. Thermodynamic equilibrium between concomitant phases (brine– N_2) is calculated at each time step to evaluate the water vapor fraction in the gas and the dissolved gas in the brine.

A 1D column model 6 cm long was used as a conceptual framework for determining the evolution of the water content induced by the injection of N_2 , in both time and space. The column was represented by 10 gridblocks composing the model mesh. The thickness of each grid cell was constant (0.6 cm). The matrix rock was assumed inert with respect to N_2 , i.e., without chemical reactivity. The dependence of relative permeability and capillary pressure on the water saturation are given in Figure 5. The relative permeability of the aqueous (k_{r1}) and gaseous (k_{r2}) phases, and the capillary pressure (P_{cap}) are described by the relevant van Genuchten (1980) equations.

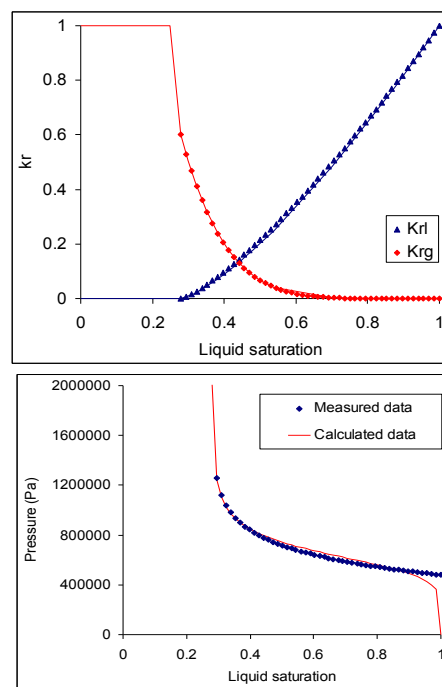


Figure 5. Relative permeability and capillary pressure curve according to water saturation (S_l).

Due to the low permeability of the medium, the model predictions are very sensitive to the relative permeability and capillary pressure characteristics, in particular to the entry pressure. As shown by Figure 5, the van Genuchten (1980) model does not fit the measured data adequately when the liquid saturation is close to 1. This very weak shift has an impact on the breakthrough time.

For the "Grès de Molière" rock, high-pressure mercury injection and standard centrifugation were used to measure the capillary pressure curve. The model parameters are: $S_{lr} = 0.22$, $S_{gr} = 0.05$, $P_0 = 645161$ Pa and $m = 0.95$. When these parameters are correctly defined, the code can reproduce, with good agreement, the first three stages of the experiment, including the mean water saturation and the outlet gas flow rate (Figure 5).

These three first stages correspond to the desaturation of the porous medium according to a classical piston effect. The desaturation state is proportional to the pressure gradient applied to the core, whereas the evaporation process is negligible: at the end of stage 3, the water content is close to the residual liquid saturation.

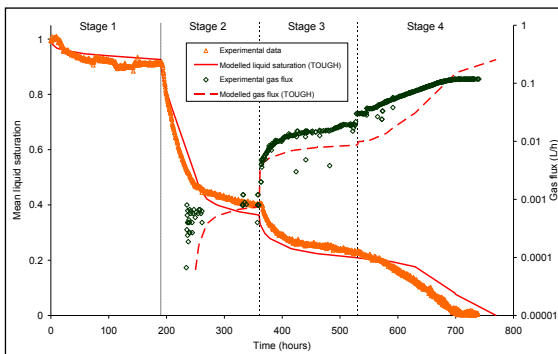


Figure 6. Results of dryout experiments with gaseous N_2 at laboratory scale (Peysson et al., 2010) compared with results from the numerical modeling performed with the TOUGH2 code (André et al. 2010).

During the first three stages, the calculated average water saturation in the core fits the measured data well. Some discrepancies are observed close to the inlet and outlet of the column, resulting mainly from the choice of parameters describing the boundary conditions imposed on the numerical model.

The last stage (stage 4) corresponds to the desiccation of the medium. Even if the global tendency is roughly reproduced, this stage presented some difficulties in reproducing correctly the measured data.

The only way to adequately fit both gas flow rate and desiccation time was to increase the gas permeability when liquid saturation was lower than the residual liquid saturation. By increasing the relative gas permeability, the outlet gas flow rate grows; the evaporation process goes faster and the time needed to totally desiccate the core decreases. These numerical simulations of laboratory experiments at $90^\circ C$ not only served to check the relevance of the model, but they also helped in determining the parameters of the integrated approaches with the highest sensitivity (i.e., the optimized relative permeability and capillary pressure curves). The good agreement between measured and calculated data is very encouraging. We also demonstrated that the petrophysical parameters established at $90^\circ C$ are applicable at $120^\circ C$ without any adjustment for the same rock (André et al., 2010).

Extrapolation at field scale (2D-radial approach)

Because of gravity forces and the supercritical CO_2 density (lower than that of the brine), the reservoir desaturates faster at the top when extrapolated to the near-wellbore field. Figure 7 clearly shows that the porous medium has dried to a radius of about 12 m at the reservoir top, whereas at the bottom, only the first meter around the well is totally desiccated. Inside the drying zone, solid salt (i.e., halite) precipitates. If salt is present anywhere in the entire desaturated zone, the spatial repartition of salt deposits varies, according to the resultant prevalent transport forces (advection, diffusion, capillary, evaporation, etc.) inside the reservoir: the amounts are higher at the bottom of the reservoir, and lower at the top, for the simulation conditions and the specific characteristics of the reservoir in this study. The pattern of solid saturation (= solid volume/pore volume) distribution indicates that 40% of the porosity is occupied by salt at the bottom, whereas only 10% at the top is filled. The porosity and, consequently, the permeability are more impacted at the bottom of the reservoir (Figure 8). The permeability decrease is represented by the empirical function $k_{red} (= k/k_0)$. This function clearly shows that largest permeability reductions are

expected close to the well (the skin effect in the first cell next to the well) and at the lower part of the reservoir (in the first meter above the base of the reservoir).

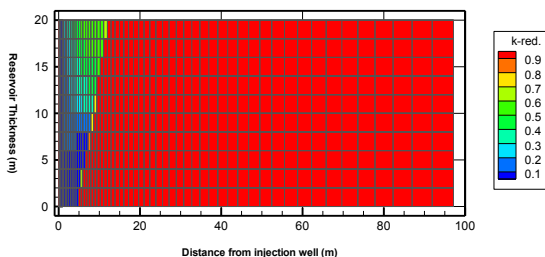


Figure 7. Permeability reduction, k_{red} ($=k/k_0$) inside a 100 m radius around the injector well after ten years of CO_2 injection.

Finally, we specifically investigated the influence of downtime during the storage phase of well injectivity. Numerical simulations were performed considering the case of CO_2 injection into an aquifer open with a nominal flow of $1MMm^3/y$ and several short shutdown periods. Pc-Kr models were built to be fully representative of rock types with permeabilities of 10 and 100 mD for an integrated approach ensuring consistency between original K, K_r , and Pc. So far, the results show little effect related to re-imbibition layers. The temporary shutdown of the wells does not seem to pose a major problem with respect to injectivity in the homogeneous model even when including hysteretic effects.

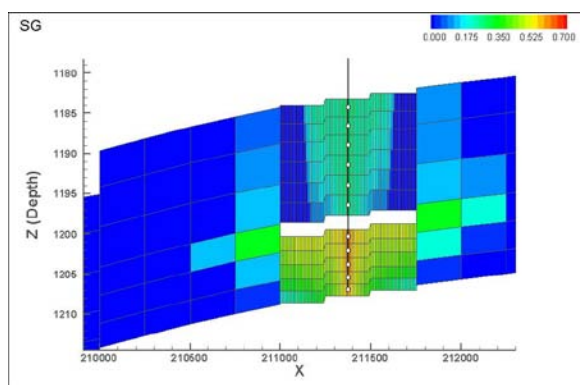


Figure 8. Vertical section illustrating the saturation tank of gas around the injection well for a mid-horizontal permeability 100 mD (RT1) in the deep layers and 10 mD (RT2) in the upper layers. This saturation state is the last day of the injection history, after six years of injections interrupted by two years of rest.

CONCLUSIONS

For the flows in the wells, the numerical simulation results show trends highlighting the problem of an “injectivity gap,” showing an inability to maintain a controllable pressure range at the bottom of the injection well because of phase changes in that well. The involvement of industry (i.e., Schlumberger, GDF Suez, and Total) in the project contributes validated injection scenarios.

Most of our efforts to study the mechanisms at the interfaces of geochemical phases (CO_2 sc-brines) were focused on CO_2 solubility in capillary water. Detailed speciation of carbonic acid is well established for the range of relative humidity and drying conditions studied in the project. A comprehensive approach for estimating the interfacial tension of a brine- CO_2 sc system based on the theory of electrolytic systems was developed (Leroy et al., 2010).

We investigated the drying processes through laboratory experiments and numerical simulations to evaluate the dynamic of the water-saturation decrease in sandstones and the consequences of induced salt depositions on injectivity. We demonstrate that in low-permeability porous media, the relative permeability of the gas phase significantly increases when water saturation is lower than the irreducible water saturation. When this parameter is adjusted, the numerical code is able to reproduce the drying time and the outlet gas flow rate measured at laboratory scale on cores, using a two-phase Darcy flow and thermodynamic equilibrium between phases.

At field scale, the rock characteristics defined at laboratory scale are used to predict the behaviour of the near-well zone according to the injection gas flow rate. We demonstrated that the precipitation process and the amount of salt deposits are related to different parameters:

- The salinity of the initial brine: The more concentrated the brine, the more massive the salt deposit.
- The irreducible water content: water entrapped in pores is evaporated by gas injection.

tion. The higher this content, the more important the amount of precipitated salt.

- The gas injection flow rate and the capillary forces within the system.

Finally, all these parameters have to be known (and defined) in order to improve the management of the long-term injection of CO₂ into saline aquifers. According to reservoir simulations already conducted, several important results can be noted:

1. For high permeabilities (>100 mD), aquifer rewetting is more extensive, but no impact is observed in terms of injectivity because of the high permeability;
2. For low permeabilities (<100 mD), re-imbibition is less extensive and may have an adverse impact on well injectivity after restart;
3. Heterogeneities do not appear to play a major role in these findings
4. The key parameter is the curve of relative permeability to water. It is therefore recommended to measure this parameter accurately during the design phase.

ACKNOWLEDGMENT

This work is carried out within the framework of the “*Proche Puits*” project, co-funded by the French National Agency for Research (ANR). The authors are grateful to all project partners (TOTAL, GDF Suez, Schlumberger, Itasca, CNRS, University of Lorraine, and University of Pau) for allowing the publication of this work.

REFERENCES

- André L., P. Audigane, M. Azaroual, and A. Menjoz, Numerical modeling of fluid-rock chemical interactions at the supercritical CO₂-liquid interface during supercritical carbon dioxide injection into a carbonated reservoir, the Dogger aquifer (Paris Basin, France). *Energ. Conv. Manage.*, 48, 1782-1797, 2007.
- André, L., M. Azaroual, and A. Menjoz, Numerical Simulations of the Thermal Impact of Supercritical CO₂ Injection on Chemical Reactivity in a Carbonate Saline Reservoir. *Transp. Porous Med.*, 82, 247-274, 2010.
- Gaus I., M. Azaroual, and I. Czernichowski-Lauriol, Reactive transport modelling of the impact of CO₂ injection on the clayey caprock at Sleipner (North Sea). *Chem. Geol.*, 217, 319-337, 2005.
- Incropera F.P., De Witt D.P., (2001) Fundamentals of heat & mass transfer (5th edition), John Wiley and Sons, 980p.
- Leroy, P., Lassin, A., Azaroual, M., and André, L., (2010). Predicting the surface tension of aqueous 1:1 electrolyte solutions at high salinity. *Geochimica et Cosmochimica Acta* 74, 5427-5442.
- Oldenburg C.M., Moridis G.J., Spycher N., Pruess K., 2004. EOS7C Version 1.0: TOUGH2 Module for Carbon Dioxide or Nitrogen in Natural Gas (Methane) Reservoirs. *Lawrence Berkeley National Laboratory Report LBNL-56589*, Berkeley, CA (USA).
- Pruess K., C.M. Oldenburg, and G.J. Moridis, TOUGH2 User's Guide, Version 2.0. *Lawrence Berkeley National Laboratory Report LBNL-43134*, Berkeley, CA (USA), 1999.
- Verma A., and K. Pruess, Thermohydrologic conditions and silica redistribution near high-level nuclear wastes emplaced in saturated geological formations, *J. Geophys. Res.*, 93(B2), 1159–1173, 1988.
- Xu T., and K. Pruess, Modeling multiphase non-isothermal fluid flow and reactive geochemical transport in variably saturated fractured rocks: 1. Methodology, *Am. J. Sci.*, 301, 16-33, 2001.
- Peysson Y., Bazin B., Magnier C., Kohler E., Youssef S., 2010. Permeability alteration due to salt precipitation driven by drying in the context of CO₂ injection. International Conference on Greenhouse Gas Technologies (GHGT-10), Amsterdam, 19-23 September 2010.
- Mahadevan J., 2005. Flow-through drying of porous media. *PhD Dissertation*. The University of Texas at Austin.
- Mahadevan J., Sharma M.M., Yortsos Y.C., 2007. Water removal from porous media by gas injection: experiments and simulation. *Transport in Porous Media*, 66, p. 287-309.
- Kleinitz W., Dietzsch G., Köhler M., 2003. Halite scale formation in gas producing wells. *Chemical Engineering Research and Design* 81 (PartA).
- Zeidouni M., Pooladi-Darvish M., Keith D., 2009. Analytical solution to evaluate salt precipitation during CO₂ injection in saline aquifers, *International Journal of Greenhouse Gas Control*, 3, p. 600–611